JOC The Journal of Organic Chemistry

ARTICLE

pubs.acs.org/joc

Synthesis, Characterization, and Applications of Hemifluorinated Dibranched Amphiphiles

Maria Cristina Parlato,[†] Jun-Pil Jee,[†] Motti Teshite,[†] and Sandro Mecozzi*[,†,‡]

[†]School of Pharmacy and [‡]Department of Chemistry, University of Wisconsin—Madison, Madison, Wisconsin 53705, United States

Supporting Information

ABSTRACT: Here we describe the synthesis and the physicochemical and preliminary pharmaceutical assessment of a novel class of hemifluorinated dibranched derivatives: $M_1diH_xF_y$. These compounds have the remarkable ability to completely stop the Ostwald ripening commonly associated with nanoemulsions. The developed synthesis is modular and allows easy incremental structural variations in the fluorophilic (fluorous chains), lipophilic (alkyl spacer head), and hydrophilic (polar head) domains. Furthermore, the synthesis can be easily scaled up and highly pure compounds can be readily obtained through silica gel and fluoro-silica gel column chromatography, without any need to use HPLC or other time-consuming techniques. Surface properties such as micelle formation, critical aggregation concentration (CAC), and emulsion stability studies demonstrated the different behavior of the dibranched hemifluorinated surfactant $M_1diH_xF_y$ with respect to that of single-chain semifluorinated analogues M_zF_y. Remarkably, the new polymer $M_1diH_3F_8$ drastically slowed the ripening of nanoemulsions of the commonly used fluorinated anesthetic sevoflurane over a period of more than 1 year. During this time, the nanodroplet size did not increase to more than 400 nm. This result is very promising for inducing and maintaining general anesthesia through intravenous delivery of volatile anesthetics, eliminating the need for the use of large and costly vaporizers in the operating room.

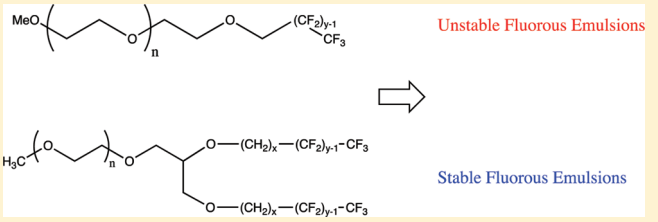

INTRODUCTION

Fluorinated amphiphiles have unique physicochemical properties, including high surface tension activity, thermal and chemical stability, and biological inertness.[1,2] The fluorous moiety is characterized by both high hydro- and lipophobicity. Furthermore, linear fluorocarbons are rigid rods due to the size of the fluorine atom. All these properties allow fluorinated amphiphiles to form better organized and more stable self-assembling systems than their hydrocarbon counterparts.[1−12] Also, important from a biological standpoint, the high lipophobicity of fluorous chains mostly prevents the fusion of these molecules with biological membranes, therefore strongly reducing their hemolytic activity and acute toxicity in comparison to their hydrocarbon analogues. Fluorocarbons are not metabolized in vivo and are eventually excreted unmodified.[13] Due to these unique physicochemical and biological properties, fluorinated amphiphiles are one of the most promising and innovative tools for the construction of drug-delivery devices and other biomedical applications.

Intravenous delivery of fluorinated volatile anesthetics with little or no aqueous solubility has been a focus area of pharmaceutical research for over 40 years, due to the potential for pharmacodynamics improvements. However, the peculiar properties of fluorous molecules have prevented a quick solution to the problem of finding formulations able to stabilize fluorous anesthetics in water. For instance, the use of lipid-based emulsions only allowed formulations containing up to 3.6% of sevoflurane, a concentration not sufficient for medical applications as an intravenous anesthetic.[14] We originally proposed the possibility of using semifluorinated surfactants for the intravenous delivery of the commonly used class of fluorinated volatile anesthetics.[15,16] We found that by using linear diblock copolymers such as the simple M_5F_{13} polymer (Figure 1), we were able to solubilize up to 25% of sevoflurane in water.

In vivo testing of these fluorous emulsions showed that both induction and recovery from intravenous emulsified halogenated anesthetics are more rapid than those with administration as a vapor.[16] Additionally, the intravenous administration of fluorinated ethers has promising implications regarding end-organ protection against ischemia and reperfusion injury.[17,18] This preconditioning is found to be a separate pharmacologic response from the drug effects that result in general anesthesia. Therefore, the potential clinical applications of intravenous emulsified fluorinated anesthetics may well extend beyond the operating room.[19] Sevoflurane, a moderately water soluble highly fluorinated ether, used for induction and maintenance of general anesthesia, is the preferred agent in clinical anesthesia, due to less irritation to mucous membranes in comparison to that for other fluorous ethers with anesthetic properties such as isoflurane and desflurane.[20,21] The affinity of fluorinated anesthetics for fluorophilic molecules prompted the investigation of the emulsification of sevoflurane using the semifluorinated surfactant M_5F_{13} (Figure 1) with the fluorinated and FDA-approved additive perfluorooctyl bromide to slow ripening. This new formulation

Received: May 2, 2011
Published: July 07, 2011

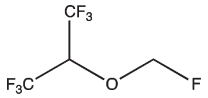

Sevoflurane **1**

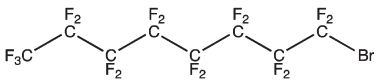

PFOB **2**

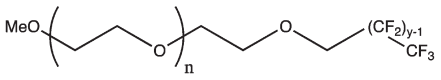

M_zF_y

3a n = 25, y = 13, M_1F_{13} (PEG MW = 1100)
3b n = 113, y = 13, M_5F_{13} (PEG MW = 5000)

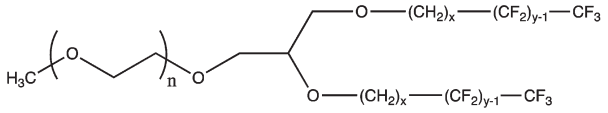

4a n=25, x=3, y=5, $M_1diH_3F_6$
4b n=25, x=3, y=7, $M_1diH_3F_8$
4c n=25, x=5, y=7, $M_1diH_5F_8$
4d n=25, x=10, y=5, $M_1diH_{10}F_6$
4e n=25, x=10, y=7, $M_1diH_{10}F_8$

Figure 1. Structures of the volatile anesthetic sevoflurane, the additive perfluorooctyl bromide, the polymer series M_zF_y, and the new polymer series $M_1diH_xF_y$. The number following the letter M indicates the molecular weight of the PEG. Thus, M5 indicates a methyl-capped poly(ethylene glycol) of average molecular weight of 5000. The number after the H indicates the number of carbon atoms composing the hydrocarbon segment, while the number after the F indicates the number of carbon atoms in the fluorocarbon chains.

allowed the emulsification of a considerable amount of sevoflurane, up to 25% v/v, by exploiting the greater solubility of the anesthetic in a fluorous phase. This was a significant improvement (6-fold increase) over the maximum amount of sevoflurane that can be emulsified in classic lipid emulsion (intralipid), 3.46% v/v.[6] Our formulations have the ability of inducing general anesthesia by intravenous injection in rats[16] and in dogs,[22] combined with a rapid recovery profile without causing acute toxicity. Nevertheless, the sevoflurane/fluoropolymer emulsions were susceptible to fast particle size growth. For any emulsion formulation to become clinically useful, the particle droplet size must be under 500 nm and have a shelf life of 18 months. The addition of perfluorooctyl bromide as a secondary component did slow the ripening, but unfortunately the droplet size was over 500 nm after just 30 days. Limiting ripening is fundamental to provide an effective and convenient means of inducing anesthesia in human patients. This problem led us to design a new class of fluorinated surfactants that could provide extended emulsion stability.

RESULTS AND DISCUSSION

Our design started from considering the structure of the nanoparticles in our emulsions. The original surfactant M_5F_{13} (**3b**; Figure 1) consisted of a large poly(ethylene glycol) with an average molecular weight of 5000 attached to a relatively small rigid perfluorocarbon. Thus, presumably, the surfactant chains would coat the fluorous nanoparticle composed of the anesthetic **1** and the additive **2** by binding the fluorous chain to the inner fluorous core. The distance between the various surfactant molecules on the surface of the nanoparticle would then be dictated by the steric hindrance of the large poly(ethylene glycol) moieties. In the case of the original polymer M_5F_{13} the large PEG would prevent tight packing of the surfactant around each nanoparticle (Figure 2).

Loose packing between the surfactant molecules surrounding the nanoparticles would then allow anesthetic molecules to diffuse into the aqueous phase and contribute to the growing of larger particles by the Ostwald ripening effect. We reasoned that, by reducing the PEG size and by increasing the volume of the fluorous moiety, we might surround each droplet with a more dense, less penetrable polymeric layer and, as a consequence, reduce the rate of diffusion of the anesthetic out of the nanoparticles (Figure 2). According to this design, we selected a PEG with an average molecular weight of 1000 as opposed to the PEG 5000 of the original polymer, and we transformed the single fluorocarbon chain we used in M_5F_{13} into two hemifluorinated chains connected to the PEG polar chain through a glycerol moiety. In addition, we introduced a small hydrocarbon segment between the two fluorous chains and the glycerol moiety to provide some flexibility to the surfactant fluorous moieties.

We herein describe the synthesis and the preliminary physicochemical and pharmaceutical assessments of this new class of nonionic dibranched derivatives $M_1diH_xF_y$ (Figure 1). The number following the letter M indicates the molecular weight of the PEG. Thus, M_5 indicates a methyl-capped poly(ethylene glycol) of average molecular weight of 5000. The number after the H indicates the number of carbon atoms composing the hydrocarbon segment, while the number after the F indicates the number of carbon atoms in the fluorocarbon chains. All these new surfactants were able to slow the ripening of sevoflurane emulsions, in comparison with the original linear diblock copolymers. Remarkably, the new polymer $M_1diH_3F_8$ drastically slowed nanoparticle ripening and stabilized sevoflurane emulsions over 1 year with a droplet size of under 400 nm.

Synthesis. A series of fluorinated 1,2-di-*O*-alkylglycerol-PEG amphiphiles have been synthesized on a gram scale with high purity. The final surfactants were easily purified by silica gel and fluoro-silica gel column chromatography without requiring further purification by HPLC. Their molecular structures follow a modular design that allows incremental structural variations. This design involves two small hydrocarbon chains ending with a fluorocarbon functionality. The two mixed hydrocarbon/fluorocarbon chains are then connected through a glycerol unit to a PEG (MW 1100) polar head. The various polymers in this series differ in the size of both the fluorous chain and the hydrocarbon spacer. We have used two different fluorocarbons, containing six and eight fluorinated carbons, respectively. The hydrocarbon spacer between the PEG moiety and the terminal perfluoroalkyl group contains 3, 5, or 10 methylene groups. These structural features are expected to influence the fluorophilic/lipophilic/hydrophilic balance and, consequently, physicochemical and biological properties such as nanoparticle permeability and nanoemulsion stability.

While the synthesis of dialkyl-semifluorinated amphiphiles is documented in the literature, the synthesis of PEG-containing fluorous surfactants is challenging. Our main constraint was dictated by the need for gram-scale synthesis in order to produce enough amphiphile as needed for physicochemical characterization and for all pharmaceutical and biological studies. The synthesis and purification of compounds containing fluorous moieties can be very problematic, due to their unusual reactivities,

dx.doi.org/10.1021/jo200835y |*J. Org. Chem.* 2011, 76, 6584–6591

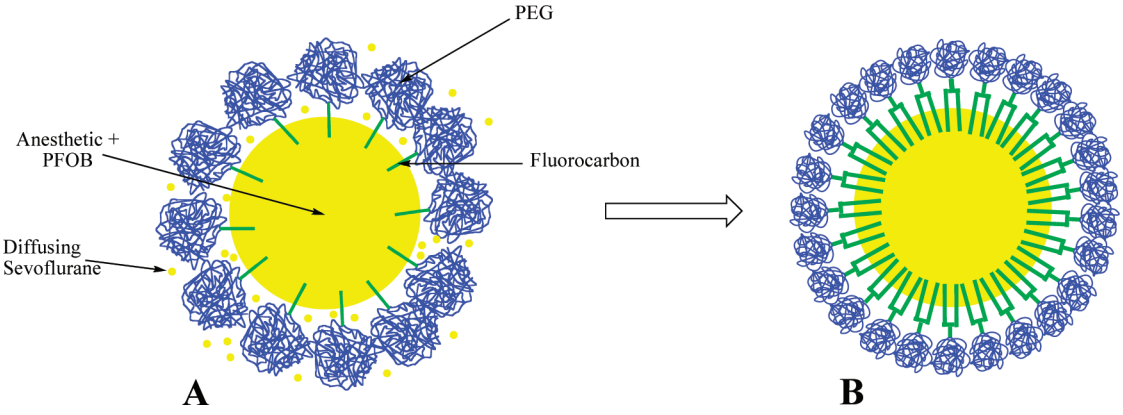

Figure 2. Rational design of stable nanoemulsions. (A) The original polymer composed of a large poly(ethylene glycol) and a single small fluorocarbon chain can self-assemble around the fluorous nanoparticle only in a loose manner, leaving spaces for the diffusion of the anesthetic out of the nanoparticle. The diffused anesthetic would then contribute to the growing of larger nanoparticles by the Ostwald ripening effect. (B) The newly designed polymers composed of a smaller PEG and a larger two-chain fluorous moiety is able to better surround the fluorous nanoparticle and strongly reduce the amount of anesthetic that can diffuse out.

Scheme 1

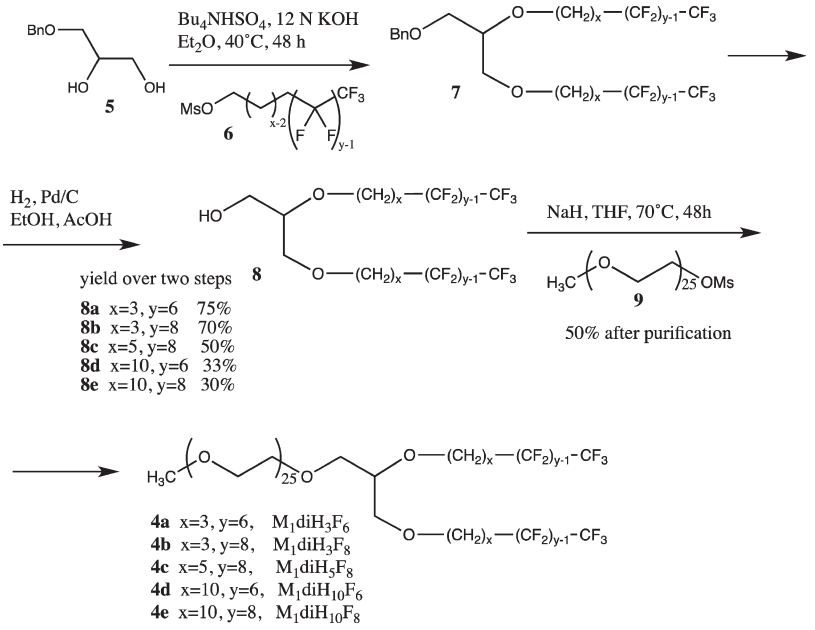

hydrophobicity, and lipophobicity, which can lead to difficulties in handling, solubilization, and purification of reagents and intermediates of reaction. All these issues are exacerbated if fluorous compounds containing reactive functionalities directly attached to the strongly electron withdrawing fluorous chains are used in the synthesis. In fact, the electron-withdrawing properties of fluorocarbons will greatly reduce the reactivity of these molecules. To improve on the reactivity of fluorous intermediates, we resorted to the use of short (up to eight carbon atoms) fluorous chains, containing a small hydrocarbon spacer between the reactive functionalities and the fluorous tails (Scheme 1). The next task consisted of identifying the conditions for a quick and easy way to purify the PEG-containing semifluorinated polymeric surfactants. Unfortunately, a mixture of different fluorous amphiphilic PEG derivatives cannot be purified by using common laboratory techniques such as silica gel column chromatography or precipitation when the PEG moiety is large compared to the hydrophobic/fluorophilic moieties. Then, the only possibility of avoiding time-consuming and expensive purification techniques such as preparative HPLC resides in the possibility of pushing to completion all reactions run on PEG-containing molecules and purifying the final product.

The synthesis of of the di-*O*-alkylglycerol precursor **7** has been reported in the literature[23] and was performed by alkylation under phase-transfer-catalysis conditions of benzyl-monoprotected *rac*-1-*O*-benzylglycerol using perfluoroalkyl mesylates, followed by hydrogenolysis for removal of the benzyl protecting group. Purification of compounds **7** would require a tedious purification by silica gel chromatography because of the close proximity of the R_f values for the mesyl alcohol **6** and derivative **7**. For this reason, we proceeded to the following hydrogenolysis after just quick filtration on a silica gel pad. The deprotected

dx.doi.org/10.1021/jo200835y |*J. Org. Chem.* 2011, 76, 6584–6591

Scheme 2

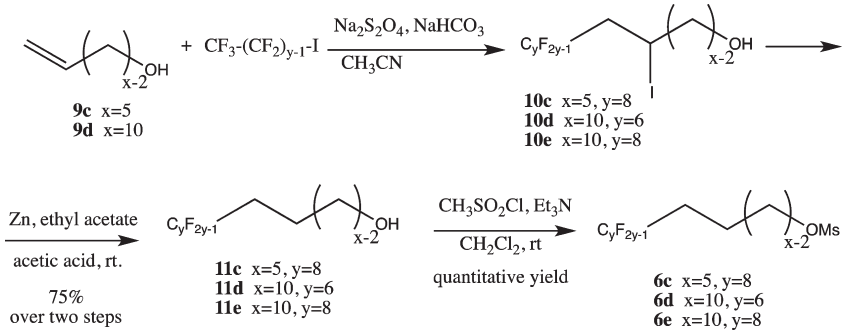

derivatives **8a**−**e** could then be easily purified from other impurities by simple silica gel column chromatography.

Several of the partially fluorinated alcohols **11** with the general structure $C_mF_{2m+1}(CH_2)_nOH$ were not commercially available. They were synthesized from 9-decen-1-ol or 4-penten-1-ol following a procedure reported in the literature.[24,25] A sequence of redox and radical reactions is used in the synthesis of these alcohols (Scheme 2).

In the last step for the synthesis of the amphiphiles (Scheme 1), the glycerol derivatives **8** were coupled with polyethylene glycol monomethyl ether (MW 1100) methanesulfonate ester by following a procedure developed in our laboratory.[8] The reactions were monitored by ^{1}H NMR spectroscopy. As shown by FT-MALDI spectra, a small amount of polyethylene glycol monomethyl ether was present in the final compound, possibly deriving from hydrolysis of the polymeric methanesulfonate ester during the coupling step. This impurity was easily removed by fluoro flash silica gel chromatography, while ordinary silica gel chromatography allowed the removal of fluorous alcohols and other side products. All steps of Schemes 1 and 2 have been performed on a gram scale with high purity (as shown from both HPLC and mass spectrometry analysis) and in good yields.

Physicochemical Characterization. All synthesized surfactants were highly soluble in water at room temperature, and the solutions were clear. Interestingly, $M_1diH_3F_8$ gave a high-viscosity solution that was, however, still suitable for emulsion preparation. Fluorinated surfactants are characterized by higher hydrophobicity and start to aggregate at a relatively lower concentration than the corresponding hydrogenated compounds. Furthermore, they form better organized and more stable structures than their hydrocarbon counterparts. Such interesting properties mainly result from the stiff structure of the fluorocarbon chain, which is bulkier and more rigid than a hydrocarbon.[1] We initially expected amphiphiles **4a**−**e** to form micelles in aqueous solution. Dynamic light scattering was applied to measure the average size of the amphiphilic aggregates in solution. The particle size data are summarized in Table 1. Interestingly, the size of the aggregates made by the various polymers radically changes on the basis of very small changes in the structure of the polymers. For instance, the average nanoparticle size doubles when $M_1diH_3F_8$ is used in place of $M_1diH_3F_6$. The aggregate size reaches the remarkable value of about 113 nm with $M_1diH_{10}F_8$. In comparison, the micellar aggregate made by a linear diblock copolymer such as M_1F_{13} is just 17 nm, as expected. The much larger size of the aggregates made by the dibranched polymers suggests that aggregates other than micelles are actually formed. The size and

Table 1

polymer	particle size (nm)[a]	CAC (M)
M_1F_{13}	17.17 ± 1.85	5.50×10^{-7}
M_5F_{13}	17.23 ± 3.73	7.94×10^{-7}
$M_1diH_3F_6$	36.45 ± 1.64	9.91×10^{-6}
$M_1diH_3F_8$	80.53 ± 7.93	6.11×10^{-6}
$M_1diH_5F_8$	81.48 ± 15.17	5.45×10^{-6}
$M_1diH_{10}F_6$	83.66 ± 13.58	not available
$M_1diH_{10}F_8$	112.93 ± 1.83	7.22×10^{-7}

[a] Particle sizes of fluoropolymer-based aggregates. Data are given with the standard deviation. Each measurement was repeated three times (n = 3).

shape formed by self-assembling amphiphiles are dictated by the ratio of the volumes between the hydrophilic moiety and the hydrophobic moiety. In the case at hand, a relatively small PEG (MW 1100, corresponding to 25 ethylene glycol units) is attached to a wide hydrophobic tail composed of two different chains. This combination may in principle lead to the formation of various aggregates, from cylindrical micelles to vesicles and bilayer structures in general. A transmission electron microscopy study of the aggregates made by the polymer $M_1diH_{10}F_6$ in aqueous solution showed a variety of particles of different sizes and shapes, suggestive of the formation of various bilayer structures (see the Supporting Information). It is important to recognize that the ability of a surfactant to form either a micelle or other structures does not have any effect on its ability in stabilizing a nanoemulsion. As a matter of fact, the same geometric features that in polymer $M_1diH_{10}F_6$ make impossible the formation of micelles, namely a relatively small hydrophilic head and a wide hydrophobic tail, are also the reasons we expected an improved stabilization of the corresponding nanoemulsions. Wider hydrophobic and fluorophilic tails would pack better around the fluorophilic nanodroplets, and a smaller PEG (from M_5 to M_1) would reduce the spaces between the polymeric chains surrounding the nanodroplets, thus reducing the diffusion of the anesthetic out of the nanodroplet core.

The critical aggregate concentrations (CAC) of the new polymers were estimated by measuring the surface tension of polymer solutions at various concentrations. Increasing the concentration of the polymer under the CAC leads to a linear decrease in the surface tension. When the CAC is reached, the surface tension no longer changes and a plateau value is reached. The CAC can be quickly estimated by the intersection between the plateau line and the line formed by the points in which a linear decrease in surface tension is observed. The CAC data presented

dx.doi.org/10.1021/jo200835y |J. Org. Chem. 2011, 76, 6584–6591

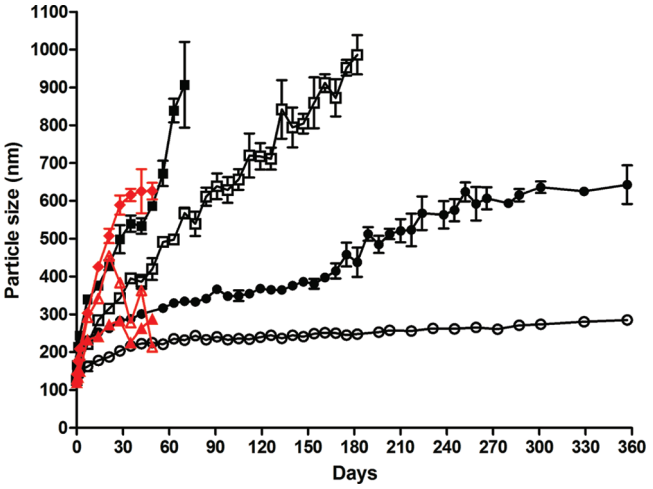

Figure 3. Change in the particle sizes of fluoropolymer-based emulsions with time: (■) M_5F_{13}-based emulsion; (□) M_1F_{13}-based emulsion; (●) $M_1diH_3F_6$-polymer-based emulsion; (○) $M_1diH_3F_8$-based emulsion; (▲) $M_1diH_5F_8$-polymer-based emulsion; (△) $M_1diH_{10}F_6$-based emulsion; (◆) $M_1diH_{10}F_8$ based emulsion. The particle size was measured over 357 days. Data are given with standard deviation ($n = 3$). Data for the last three emulsions are shown in red. These emulsions led to phase separation after 50 days. Accordingly, particle size measurements were halted after that time. All emulsions contained 20% of sevoflurane and 10% of perfluoroctyl bromide and were prepared in saline (0.9% w/w NaCl).

in Table 1 clearly show the influence of small changes in the polymer structure on the kinds of aggregates that are formed in aqueous solution. This solution behavior agrees with what is known about different nonionic surfactants.[26,27]

Emulsion Stability. In a previous article[16] we have reported on a novel anesthetic intravenous formulation composed of (1) 20% w/v of a semifluorinated surfactant, (2) 10% v/v perfluorooctyl bromide (PFOB), an FDA-approved fluorous additive, and (3) 20% v/v of a fluorinated anesthetic. This formulation could be emulsified and the corresponding nanoemulsion could be used for the intravenous delivery of the volatile anesthetic. The additive perfluorooctyl bromide increased the stability of the emulsion due to its fluorophilicity and its reduced water solubility. In principle, the slow diffusion of this secondary less water soluble component will lead to a heterogeneous distribution with smaller droplets enriched in the less soluble component and larger droplets enriched in the more soluble component. However, the osmotic pressure will limit composition differences between droplets and equilibrium will eventually be reached. This same formulation has been used for studying the stability of nanoemulsions formed by the new polymers $M_zdiH_xF_y$. Dynamic light scattering was used to measure the change in size of the droplets with time. The linear diblock copolymer M_1F_{13} was used as a benchmark.

As shown in Figure 3, the emulsions formed by the new dibranched polymers initially show a trend similar to that observed with M_1F_{13}. However, after an initial equilibration time, the nanoparticle size stabilized and ripening was reduced.

The observed trends show that Ostwald ripening is still causing an increase in the nanoparticle size, but there is an impressive decrease in the rate of particle growth. The growing rate was higher for polymers with larger intermediate alkyl chains, while it was smaller for polymers with larger fluorinated chains. As shown in Figure 3, the new polymer $M_1diH_3F_8$ very remarkably slowed the ripening and stabilized sevoflurane emulsions over 1 year. Furthermore, the droplet size stayed under 400 nm and there was no visual evidence of either phase separation or sedimentation. In comparison, the linear diblock copolymers M_5F_{13} and M_1F_{13} showed droplet sedimentation after only 30 and 60 days, respectively. These stability studies were reproduced with three more identical emulsions containing $M_1diH_3F_8$, which were followed in terms of nanoparticle size for 1 year. All emulsions showed identical stabilities. Thus, the use of dibranched semifluorinated surfactants allowed us to prepare nanoemulsions that are stable for extended times. The stability of these emulsions is consistent with a shelf life acceptable for clinical use.

CONCLUSIONS

A novel class of hemifluorinated dibranched PEG-based surfactants was synthesized. The purification of PEG-containing fluorous molecules can be very difficult. The value of the developed synthesis lies in the possibility of obtaining surfactants on a gram scale with high purity by using simple purification techniques such as simple silica gel and fluoro flash silica gel column chromatography. The synthesis of these surfactants has been developed with a modular approach, which easily allows incremental structural variations in the fluorophilic, hydrophobic, and hydrophilic domains. The relative ratio of the three molecular domains affects the hydrophobic/hydrophilic balance, leading to the possibility of tuning physicochemical (stability, fluidity/rigidity, permeability) and biological properties.

Surface properties such as the critical aggregate concentration and the nanoemulsion stability were found to be affected by the size of both the perfluorinated tail and the hydrogenated spacer, demonstrating the peculiar behavior of dibranched hemifluorinated surfactants with respect to single-chain perfluorinated analogues. All the newly synthesized dibranched surfactants were able to stabilize nanoemulsions containing the fluorinated anesthetic sevoflurane and the additive perfluorooctyl bromide better than linear diblock copolymers such as M_1F_{13}. Remarkably, the new polymer $M_1diH_3F_8$ dramatically slowed the ripening and stabilized sevoflurane emulsions over 1 year with a droplet size of under 400 nm. The stabilization of nanoemulsions for an extended period of time is usually very difficult. The fact that the new polymers were able to achieve exactly this feat is indicative of their potential for clinical use.

EXPERIMENTAL SECTION

Dry reactions were performed under argon using dry solvents and reagents. Perfluorooctyl iodide, 1-iodoperfluorohexane, and perfluoro alcohols were purchased from SynQuest Laboratories. Methylene chloride and tetrahydrofuran were dried by flowing through alumina-containing columns. Acetonitrile, dry diethyl ether, and methanol were used as provided. Column chromatography: silica gel 60 (Merck, 70−23 mesh), fluorous flash silica gel (Merck, 70−23 mesh).

HPLC chromatograms for product purity determination were obtained using a Jordi RP-DVB column with a particle size of 5 μm and pore size of 1000 Å. The solvent gradient started at 10% acetonitrile/90% water and increased to 100% acetonitrile over 25 min. The flow rate was 1 mL/min.

General Procedures for Perfluorinated Alcohols 11c−e.[24,25]**-** *Compound* ***10e***. Perfluorooctyl iodide (3.28 g, 6.00 mmol), $NaHCO_3$ (431 mg, 5.04 mmol), and 85% $Na_2S_2O_4$ (1.03 g, 5.04 mmol) were added at 0 °C to a solution of 9-decen-1-ol (787 mg, 5.04 mmol) in CH_3CN

dx.doi.org/10.1021/jo200835y |J. Org. Chem. 2011, 76, 6584–6591

(15 mL) and deionized H_2O (5 mL). This mixture was stirred for 4 h at room temperature. The mixture was diluted with deionized H_2O and then extracted with dichloromethane. The organic layers were washed with saturated aqueous NaCl and then dried over $MgSO_4$. After filtration and rotary evaporation of the solvent, the residue was used as a crude compound in the next step. ^{1}H NMR ($CDCl_3$): δ 1.27−1.41 (8H, m), 1.53−1.58 (4H, m), 2.01−2.07 (2H, m), 3.64 (2H, t, J = 6.8 Hz, H1), 4.91−5.02 (2H, m), 5.76−5.86 (1H, m).

Compound ***11e***. The crude compound (5.04 mmol) was dissolved in glacial acetic acid (3 mL); then zinc dust was added (988 mg, 15.12 mmol) and the mixture was stirred for 16 h at room temperature. After filtration and evaporation of the solvent, the residue was purified by column chromatography (EtOAc 70%/*n*-hexane 30%) to yield the desired compound as a white solid (2,36 g, 75%). ^{1}H NMR ($CDCl_3$): δ 1.29−1.37 (12H, m), 1.53−1.63 (4H, m), 1.98−2.11 (2H, m), 3.64 (2H, J = 6.8 Hz).

Compound ***10c***. ^{1}H NMR ($CDCl_3$): δ 1.64−1.73 (2H, m, H3), 1.74−1.99 (2H, m, H2), 2.73−3.01 (1H, m, H5), 3.72 (2H, t, J = 6.4 Hz, H1), 4.35−4.42 (1H, m, H4).

Compound ***11c***. This compound was prepared with 4-penten-1-ol and perfluorooctyl iodide: white solid, 83% yield. ^{1}H NMR ($CDCl_3$): δ 1.44−1.51 (2H, m), 1.59−1.67 (4H, m, H2), 2.01−2.08 (2H, m), 3.69 (2H, t, J = 6.4 Hz).

Compound ***10d***. ^{1}H NMR ($CDCl_3$): δ 1.26−1.43 (8H, m), 1.55−1.58 (4H, m), 1.73−1.89 (2H, m), 3.62−3.67 (2H, m), 4.09−4.13 (2H, m), 4.31−5.37 (1H, m).

Compound ***11d***. This compound was prepared with 9-decen-1-ol and 1-iodoperfluorohexane: pale oil, 80% yield. ^{1}H NMR ($CDCl_3$): δ 1.18−1.23 (12H, m), 1.44−1−56 (4H, m), 1.90−1.97 (2H, m), 3.54 (2H, J = 6.8 Hz).

General Procedure for Mesyl Derivatives 6a−e. Mesyl chloride (1.3 equiv) was added at 0 °C to a solution of alcohol **11** in dry DCM and Et_3N (2.4 equiv). The reaction mixture was warmed to room temperature and was then stirred under argon for 16 h. The mixture was diluted with dichloromethane and washed with water. The organic layers were dried over $MgSO_4$. After filtration and evaporation of the solvent, the residue was used in the next step without further purification. Quantitative yield (from ^{1}H NMR). **6c**−**e** were obtained as white solids and **6a**,**b** as pale oils.

Compound ***6a***. ^{1}H NMR ($CDCl_3$): δ 1.80−2.24 (2H, m), 2.60−2.28 (2H, m), 2.94 (3H, s), 4.23 (2H, t, J = 6.40 Hz).

Compound ***6b***. ^{1}H NMR ($CDCl_3$): δ 2.05−2.13 (2H, m), 2.19−2.32 (2H, m), 3.05 (3H, s), 4.32 (2H, t, J = 5.8 Hz).

Compound ***6c***. ^{1}H NMR ($CDCl_3$): δ 1.49−1.57 (2H, m, H3), 1.63−1.71 (2H, m, H4), 1.77−1.84 (2H, m, H2), 2.03−2.16 (2H, m, H5), 3.01 (3H, s, CH_3), 4.25 (2H, t, J = 6.4 Hz, H1).

Compound ***6d***. ^{1}H NMR ($CDCl_3$): δ 1.30−1.40 (12H, m, H3, H4, H5, H6, H7, H8), 1.56−1.63 (2H, m, H9), 1.72−1.79 (2H, m, H2), 1.98−2.12 (2H, m, H10), 3.03 (3H, s, CH_3), 4.23 (2H, t, J = 6.4 Hz, H1).

Compound ***6e***. ^{1}H NMR ($CDCl_3$): δ 1.29−1.40 (12H, m, H3, H4, H5, H6, H7, H8), 1.56−1.62 (2H, m, H9), 1.71−1.78 (2H, m, H2), 1.98−2.12 (2H, m, H10), 3.00 (3H, s, CH_3), 4.23 (2H, t, J = 6.8 Hz, H1).

Benzylated Glycerol Derivatives Bn-diH_xF_y. To a solution of F_yH_xOM (**6**; 11 mmol) and **5** (5.5 mmol) in 35 mL of Et_2O was added a solution of 12 N KOH (20 mL) and $Bu_4N(HSO_4)$ (0.05 equiv). The mixture was heated for 48 h under reflux conditions. The aqueous phase was extracted with Et_2O, and the combined organic phases were washed, dried, and rotary evaporated. The residue was purified by silica gel chromatography (petroleum ether/ethyl acetate 7/3).

Compound ***7a***. Pale oil, 85% yield. Mass (MALDI): calcd for $[C_{28}H_{24}F_{26}O_3 + Na]^+$ 925.120 25, found 925.124 52. R_f = 0.72 (hexane/ethyl acetate 7/3 v/v). ^{1}H NMR ($CDCl_3$): δ 1.81−1.91 (4H, m), 2.08−2.26 (4H, m), 3.47−4.53 (9H, m), 4.54 (2H, s), 7.25−7.36 (5H, m). ^{13}C NMR ($CDCl_3$) δ: 21.0 (d), 27.9 (t), 69.0, 69.8, 70.1, 71.2, 73.5 (2C), 79.0 (2C), 109.0 (2C), 111.4 (2C), 114.1 (2C), 116.1 (2C), 119.0 (2C), 121.8 (2C), 127.6 (2C), 127.8, 128.4 (2C), 138.5. ^{19}F NMR ($CDCl_3$): δ −82.4 (3F), −115.5 (2F), −123.0 (2F), −124.0 (2F), −124.4 (2F), −127.4 (2F).

Compound ***7b***. White solid, 83% yield. Mass (MALDI): calcd for $[C_{32}H_{24}F_{34}O_3 + Na]^+$ 1 125.107 47, found 1 125.103 91. R_f = 0.72 (hexane/ethyl acetate 7/2 v/v). ^{1}H NMR ($CDCl_3$): δ 1.81−1.90 (4H, m), 2.08−2.26 (4H, m), 3.47−4.54 (9H, m), 4.55 (2H, s), 7.24−7.36 (5H, m). ^{13}C NMR ($CDCl_3$): δ 21.2 (d), 28.1 (t), 69.2, 69.3, 70.1, 71.2, 70.2, 71.5, 73.7, 78.5 (2C), 109.0 (2C), 111.4 (2C), 114.1 (2C), 116.1 (2C), 119.0 (2C), 121.8 (2C), 127.9 (2C), 127.8, 128.0, 128.6 (2C), 138.4. ^{19}F NMR ($CDCl_3$): δ −81.4 (3F), −115.5 (2F), −122.4 (2F), −122.5 (2F), −123.4 (2F), −123.6 (2F), −124.3 (2F), −127.1 (2F).

Compounds ***7c***−***e***. These crude compounds were filtered through a pad of silica gel and used in the next step.

General Procedure for Hydrogenolysis. To a solution of BndiH_xF_y (7; 7.2 mmol) in ethanol (50 mL) and acetic acid (0.7 mL) was added Pd/C (0.85 g of a 19% mixture), and the reaction mixture was stirred under a hydrogen atmosphere (1.5 atm) at room temperature for 48 h. The mixture was then filtered, the solvent was rotary evaporated, and the residue was purified by silica gel chromatography (petroleum ether/ethyl acetate 6/4).

Compound ***8a***. Pale oil, 75% yield over two steps. Mass (MALDI) calculated for $[C_{21}H_{18}F_{26}O_3 + Na]^+$: 835.0733, found 835.07218. R_F = 0.50 (hexane/ethyl acetate 6:4 *v*/*v*); ^{1}HNMR (CDCl3): δ 1.85−1.93 (4H, m), 2.10−2.26 (4H, m), 3.50−3.75 (9H, m); ^{13}CNMR ($CDCl_3$) δ: 20.9 (d) , 27.8 (t), 61.6, 63.9, 68.6, 70.1, 71.1, 72.2, 80.2, 108.8 (m), 110.8 (m), 113.6 (m), 115.9 (m), 118.7 (m), 121.6 (m); ^{19}F NMR ($CDCl_3$): δ-82.1 (3F), −115.5 (2F), −123.0 (2F) −124.0 (2F), −124.2 (2F), −127.2 (2F).

Compound ***8b***. White solid, 70% yield over two steps. Mass (MALDI) calculated for $[C_{25}H_{18}F_{34}O_3 + Na]^+$: 1035.06052, found 1035.065695. R_F = 0.53 (hexane/ethyl acetate 6:4 *v*/*v*); ^{1}HNMR ($CDCl_3$): δ 1.74−1.83 (4H, m), 2.00−2.13 (4H, m), 3.44−3.62 (9H, m); ^{13}CNMR ($CDCl_3$) δ: 21.1 (d), 28.0 (t), 62.7, 69.1, 69.1, 70.2, 71.2, 79.4, 108.8 (m), 111.0 (m), 113.7 (m), 116.1 (m), 118.7 (m), 121.6 (m), 128.3; ^{19}F NMR ($CDCl_3$): δ −81.9 (3F), −115.2 (2F), −122.5 (2F), −122.7 (4F) −123.6 (2F), −124.2 (2F), −127.1 (2F).

Compound ***8c***. White solid, 50% yield over two steps. Mass (MALDI) calculated for $[C_{29}H_{26}F_{34}O_3 + Na]^+$: 1091.12312, found 1091.12278; R_F = 0.52 (hexane/ethyl acetate 6:4 *v*/*v*); ^{1}HNMR ($CDCl_3$): δ 1.37−1.44 (4H, m), 1.52−1.61 (8H, m), 1.92−2.05 (4H, m), 2.62−2.65 (m, 1H) 3.38−3.67 (9H, m). ^{13}C NMR ($CDCl_3$) δ 20.0, 25.7, 25.8, 29.3, 29.7, 30.6, 30.8, 31.1, 62.7, 69.9, 71.0, 71.2, 79.0; 106.3 (m), 108.6 (m), 110.9 (m), 113.8 (m), 115.8 (m), 118.7 (m), 121.3 (m); ^{19}F NMR ($CDCl_3$) δ: −81.9 (3F), −115.4 (3F), −122.6 (6F), −124.0 (2F), −124.4 (2F), −127.0 (2F).

Compound ***8d***. White solid, 30% yield over two steps. Mass (MALDI) calculated for $[C_{35}H_{46}F_{26}O_3 + Na]^+$: 1031.2924, found 1031.28853. R_F = 0.51 (hexane/ethyl acetate 6:4 *v*/*v*); ^{1}HNMR ($CDCl_3$) δ 1.17−1.38 (24H, m), 1.48−1.51 (8H,m), 1.86−2.00 (4H, m), 2.8 (1H, broad peak), 3.30−3.62 (9H, m). ^{13}CNMR ($CDCl_3$): δ 20.8, 25.9, 26.1, 26.2, 29.1, 29.3, 29.4, 29.5, 29.6, 29.7, 30.1, 30.6, 30.8, 31.1 (t), 62.7, 70.4, 70.8, 71.7, 78.8,108.6 (m), 111.2 (m), 113.8 (m), 115.8 (m), 118.8 (m), 121.3 (m); ^{19}F NMR ($CDCl_3$) δ: −82.2 (3F), −115.5 (2F), −123.0 (2F), −124.1 (2F), −124.8 (2F), −127.4 (2F).

Compound ***8e***. Pale oil, 33% yield over two steps. Mass (MALDI) calculated for $[C_{39}H_{46}F_{34}O_3 + Na]^+$: 1231.27963, found 1231.284153. R_F = 0.53 (hexane/ethyl acetate 6:4 *v*/*v*); ^{1}HNMR ($CDCl_3$) δ 1.17−1.38 (24H, m), 1.47−1.51 (8H,m), 1.86−2.01 (4H, m), 2.8 (1H, broad peak), 3.33−3.62 (9H, m). ^{13}CNMR ($CDCl_3$): δ 20.2, 26.2, 29.2, 29.3, 29.4, 29.5, 29.6, 29.7, 30.2, 30.7, 31.0, 31.2, 63.1, 70.5, 71.0, 71.9, 78.7, 106.4 (m), 108.5 (m), 110.7 (m), 113.6 (m), 115.8 (m), 118.7 (m), 121.2 (m); ^{19}F NMR ($CDCl_3$) δ: −81.8 (3F), −115.2 (2F), −122.5 (2F), −122.6 (4F), −123.9 (2F), −124.4 (2F), −127.0 (2F).

dx.doi.org/10.1021/jo200835y |*J. Org. Chem.* 2011, 76, 6584–6591

General Procedure for the Synthesis of Amphiphiles 4a−e. To a solution of PEG (MW = 1100)-mesylate (0.0032 mmol, 1 equiv) and alcohol (0.0048 mmol, 1.5 equiv) was added NaH (0.015 mmol, 5 equiv). The reaction mixture was refluxed under argon and then monitored throughout the complete disappearance of the methyl group in the methanesulfonate functionality by NMR (36 h). The mixture was cooled and filtered and the solvent evaporated. The residue was purified by silica gel chromatography (dichloromethane/methanol 9/1) and then by fluoro flash column chromatography (gradient from 100% water to 100% acetonitrile). Yield: 50% after purification.

Compound ***4a***. Mass (MALDI): dispersion around 2 079.965 41. R_f = 0.62 (dichloromethane/methanol 9/1 v/v). ^{1}H NMR ($CDCl_3$): δ 1.65−1.90 (4H, m); 2.10−2.27 (4H, m), 3.38 (s, 3H), 3.38−3.57 (9H, m); 3.58−3.83 (m, PEG). ^{19}F NMR ($CDCl_3$): δ −81.3 (3F), −114.9 (2F), −122.5 (2F), −123.4 (2F), −124.0 (2F), −126.7 (2F).

Compound ***4b***. Mass (MALDI): dispersion around 2 105.505 89. R_f = 0.62 (dichloromethane/methanol 9/1 v/v). ^{1}H NMR ($CDCl_3$): δ 1.82−1.90 (4H, m); 2.10−2.26 (4H, m), 3.38 (s, 3), 3.38−3.57 (9H, m); 3.58−3.83 (m, PEG). ^{19}F NMR ($CDCl_3$): δ −81.7 (3F), −114.8 (2F), −122.2 (2F), −122.4 (4F), −123.6 (2F), −125.1 (2F), −126.5 (2F).

Compound ***4c***. Mass (MALDI): dispersion around 2 249.696 21. R_f = 0.61 (dichloromethane/methanol 9/1 v/v). ^{1}H NMR ($CDCl_3$): δ 1.43−1.49 (4H, m), 1.57−1.66 (8H, m), 2.03−2.12 (4H, m), 3.82 (s, 3H), 3.38−3.57 (9H, m), 3.58−3.83 (m, PEG). ^{19}F NMR ($CDCl_3$): δ −81.7 (3F), −117.3 (2F), −124.7 (2F), −124.7 (4F), −125.6 (2F), −126.4 (2F), −129.4 (2F).

Compound ***4d***. Mass (MALDI): dispersion around 2 257.893 99. R_f = 0.62 (dichloromethane/methanol 9/1 v/v). ^{1}H NMR ($CDCl_3$): δ 1.24−1.43 (28H, m); 1.52−1.63 (4H, m), 1.98−2.18 (4H, m), 3.38 (s, 3H), 3.38−3.57 (9H, m), 3.58−3.83 (m, PEG). ^{19}F NMR ($CDCl_3$): δ −81.2 (3F), −114.2 (2F), −122.4 (2F), −123.0 (2F), −124.0 (2F), −126.6 (2F).

Compound ***4e***. Mass (MALDI): dispersion around 2 257.893 99. R_f = 0.62 (dichloromethane/methanol 9/1 v/v). ^{1}H NMR ($CDCl_3$): δ 1.20−1.42 (28H, m); 1.54−1.61 (4H, m), 2.02−2.06 (4H, m), 3.38 (s, 3H), 3.38−3.57 (9H, m), 3.58−3.83 (m, PEG). ^{19}F NMR ($CDCl_3$): δ −81.2 (3F), −114.8 (2F), −122.1 (2F), −122.3 (4F), −123.1 (2F), −123.6 (2F), −126.5 (2F).

Preparation of Polymer Micelles. Micelles were prepared using the solvent evaporation method. the polymer was dissolved in 1 mL of methanol to achieve a final concentration of 1.0×10^{-3} M. Methanol was evaporated at 65 °C under reduced pressure on a rotary evaporator to produce a thin film of polymer. The thin film was rehydrated with 1 mL of Millipore water heated at 65 °C with gentle agitation, and the flask was rotated at room temperature for 10 min. The sample was then filtered through 0.45 μm nylon syringe filters to remove any insoluble precipitate.

Particle Size Analysis of Polymer Micelles. Particle size amalysis of polymer micelles was performed by using dynamic light scattering (Zetasizer Nano ZS, Malvern) on the micellar solutions. Each particle size analysis was run at room temperature and repeated three times. Data are reported as Z-average diameters.

Critical Aggregate Concentration. All surface tension vs concentration plots are reported in the Supporting Information.

Preparation of M_5F_{13} Stock Solution. A 94.7 mg portion was dissolved in 25 mL of Millipore water. Ten solutions at concentrations ranging from 6.77×10^{-4} to 1.2×10^{-10} M were prepared by serial dilution of the stock solution. All solutions were transferred to 20 mL disposable scintillation vials. After each solution was prepared, it was heated in a water bath at 40 °C for 2 h. After a further 24 h of equilibration at room temperature, the solutions were used for surface tension measurements.

The following concentrations were used for the other polymer surface tension measurements.

M_1F_{13} (33.8 mg) was dissolved in 25 mL of Millipore water. Nine solutions were prepared with concentrations ranging from 7.59×10^{-4} to 7.59×10^{-11} M.

$M_1diH_3F_6$ (16.9 mg) was dissolved in 25 mL of Millipore water. Twelve solutions were prepared with concentrations ranging from 8.92×10^{-5} to 4.46×10^{-11} M.

$M_1diH_3F_8$ (18.5 mg) was dissolved in 25 mL of Millipore water. Twelve solutions were prepared with concentrations ranging from 3.57×10^{-4} to 1.78×10^{-9} M .

$M_1diH_5F_8$ (19.2 mg) was dissolved in 25 mL of Millipore water. Eleven solutions were prepared with concentrations ranging from 8.92×10^{-5} to 2.43×10^{-9} M.

$M_1diH_{10}F_8$ (20.4 mg) was dissolved in 25 mL of Millipore water. Thirteen solutions were prepared with concentrations ranging from 3.57×10^{-5} to 1.78×10^{-9} M.

Surface Tension Measurements. A tensiometer equipped with a circulator for constant temperature control was used to measure surface tension. A custom round rod made of platinum with a diameter of 1.034 mm and wetted length of 3.248 mm was used. First the rod was submerged into absolute alcohol and flame-dried for 4 s. This same procedure was repeated after 4 min, after which the rod was hung on the instrument and cooled for 5 min without touching any surface. The surface tension of Millipore water was measured to make sure that the vial and rod were fully cleaned before running any polymer solution measurements. The measurements were started only after the measured surface tension value of Millipore water remained within 0.2 μm of the pure water standard value. The surface tension measurements were run from the less concentrated solution to the more concentrated solution. The surface tension at each concentration was measured four times.

Nanoemulsion Preparation. A 500 mg portion of polymer was solubilized in normal saline solution (11.9 mL). Normal saline solution was made with 0.9% (w/w) of sodium chloride. Sevoflurane (Abbott Laboratories, Chicago, IL, 3.4 mL) and perfluorooctyl bromide (SynQuest Laboratories, Inc., Alachua, FL, 1.7 mL) were added to the polymer solution. The biphasic final total volume was 17 mL. The mixture was homogenized with a high-speed homogenizer for 1 min at 21 000 rpm at room temperature. The crude emulsion made with the homogenizer was then continuously homogenized with a microfluidizer for 1 min under 5000 psi at 15 °C, achieved with a cooling bath. The resulting nanoemulsions were stored in 15 mL plastic tubes at 4 °C.

Emulsion Particle Size Analysis. The emulsion particle size was measured by dynamic light scattering. The emulsions were diluted by a factor of 300 by adding 20 μL of the emulsion to 3.0 mL of Millipore water. Each particle size analysis was run for 5 min at room temperature and repeated three times. The particle diameters were analyzed through Gaussian analysis and reported as volume-weighted average diameters. Emulsions were stored at 4 °C. The emulsion particle size was analyzed at days 0, 2, 7, 14, 21, and 28 and then every 2 weeks up to 357 days if no phase separation occurred. Day 0 is when the nanoemulsions were initially prepared.

■ ASSOCIATED CONTENT

Supporting Information. Figures giving plots for CAC determination by surface tension measurements, electron microscopy procedures and images, and NMR spectra. This material is available free of charge via the Internet at http://pubs.acs.org.

■ AUTHOR INFORMATION

Corresponding Author
*E-mail: smecozzi@wisc.edu.

■ ACKNOWLEDGMENT

The work described in this article was supported by NIG grant NIGMS 079375 to S.M. J.-P.J. acknowledges support from the Korean Research Foundation (KRF-2008-357-E00065).

■ REFERENCES

(1) Gladysz, J. A.; Curran, D. P.; Horvath, I., T. *Handbook of Fluorous Chemistry*; Wiley-VCH: Weinheim, Germany, 2004.
(2) Kirsch, P. *Modern Fluoroorganic Chemistry*; Wiley-VCH: Weinheim, Germany, 2004.
(3) Rosen, B. M.; Wilson, C. J.; Wilson, D. A.; Peterca, M.; Imam, M. R.; Percec, V. *Chem. Rev.* **2009**, *109*, 6275–6540.
(4) Kraft, M., P.; Riess, J. G. *Chem. Rev.* **2009**, *109*, 1714–1792.
(5) Riess, J. G. *Curr. Opin. Coll. Int. Sci.* **2009**, *14*, 294–304.
(6) Sawada, H. *Prog. Polym. Sci.* **2007**, *32*, 509–533.
(7) Krafft, M. P.; Riess, J. G. *Act. Chim.* **2006**, *301*, 88–92.
(8) Gladysz, John A. *Science* **2006**, *313*, 1249–1250.
(9) Krafft, M. P. *J. Polym. Sci., Part A* **2006**, *44*, 4251–4258.
(10) Krafft, M. P.; Muller, P.; Maaloum, M.; Schmutz, M.; Goldmann, M.; Fontaine, P. *Self-Assembly* **2003**, 367–373.
(11) Tomalia, D. A. *Nat. Mater.* **2003**, *2*, 711–712.
(12) Amis, E. J.; Hu, N.; Seery, T. A. P.; Hogen-Esch, T. E.; Yassini, M.; Hwang, F. *Adv. Chem.* **1996**, *248*, 278–302.
(13) Krafft, M. P.; Riess, J. G. *J. Polym. Sci.* **2007**, *45*, 1185–1198.
(14) Zhou, J.; Luo, N.; Liang, X.; Liu, J. *Anesth. Analg.* **2006**, *102*, 129–34.
(15) Hoang, K. C.; Mecozzi, S. *Langmuir* **2004**, *20*, 7347–7350.
(16) Fast, J. P.; Perkins, M. G.; Pearce, R. A.; Mecozzi, S. *Anesthesiology* **2008**, *109*, 651–656.
(17) Hu, Z.-Y.; Luo, N.-F.; Liu, J. *Can. J. Anesth.* **2009**, *56*, 115–125.
(18) Chiari, P. C.; Pagel, P. S.; Tanaka, K.; Krolikowski, J. G.; Ludwig, L. M.; Trillo, R. A.; Puri, N.; Kersten, J. R.; Warltier, D. C. *Anesthesiology* **2004**, *101*, 1160–1166.
(19) Raphael, J.; Lynch, C. *Can. J. Anaesth.* **2009**, *56*, 91–5.
(20) Rudolph, U.; Antkowiak, B. *Nat. Rev. Neurosci.* **2004**, *5*, 709–20.
(21) Preckel, B.; Bolten, J. *Best Pract. Res. Clin. Anaesth.* **2005**, *19*, 331–348.
(22) Johnson, R. A.; Simmons, K. T.; Fast, J. P.; Schroeder, C. A.; Pearce, R. A.; Albrecht, R. M.; Mecozzi, S. *J. Pharm. Sci.* **2011**, *100*, 2685–2692.
(23) Ravily, V.; Gaentzler, S.; Santaella, C.; Vierling, P. *Helv. Chim. Acta* **1996**, *79*, 405–425.
(24) Takai, K.; Takagi, T.; Baba, T.; Kanamori, T. *J. Fluor. Chem.* **2004**, *125*, 1959–1964.
(25) Gopala, P.; Andruzzi, L.; Li, X.; Ober, C. K. *Macromol. Chem. Phys.* **2002**, *203*, 1573–1583.
(26) Matsuoka, K.; Yonekawa, A.; Ishii, M.; Honda, C.; Endo, K.; Moroi, Y.; Abe, Y.; Tamura, T. *Colloid Polym. Sci.* **2006**, *285*, 323–330.
(27) Sadtler, V. M.; Giulieri, F.; Krafft, M. P.; Riess, J. G *Chem. Eur. J.* **1998**, *4*, 1952.